Space charge and quantum effects on electron emission

Kevin L. Jensen, Joel Lebowitz, Y. Y. Lau, and John Luginsland

Related Articles

Shot noise of low energy electron field emission due to Klein tunneling
J. Appl. Phys. 112, 016104 (2012)

Direct observation and mechanism of increased emission sites in Fe-coated microcrystalline diamond films
J. Appl. Phys. 111, 124309 (2012)

Low threshold field emission from high-quality cubic boron nitride films
J. Appl. Phys. 111, 093728 (2012)

Screened field enhancement factor for a tall closely spaced array of identical conducting posts and implications for Fowler-Nordheim-type equations
J. Appl. Phys. 111, 096102 (2012)

Field dependence of the E1′ and M3′ electron traps in inductively coupled Ar plasma treated n-Gallium Arsenide
J. Appl. Phys. 111, 093703 (2012)

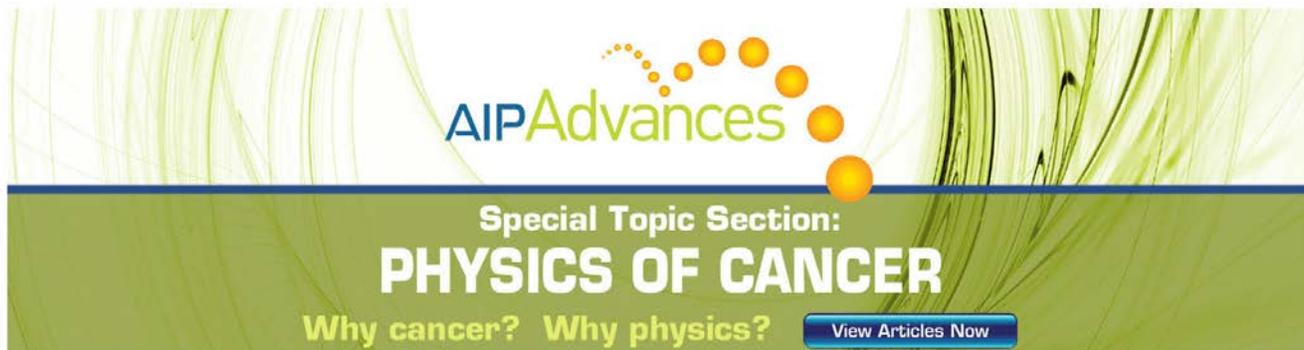## Additional information on J. Appl. Phys.

Journal Homepage: http://jap.aip.org/

Journal Information: http://jap.aip.org/about/about_the_journal

Top downloads: http://jap.aip.org/features/most_downloaded

Information for Authors: http://jap.aip.org/authors

Space charge and quantum effects on electron emission

Kevin L. Jensen,[1,a)] Joel Lebowitz,[2] Y. Y. Lau,[1,3] and John Luginsland[4]
[1]*Code 6843, Naval Research Laboratory, Washington, DC 20375, USA*
[2]*Department of Mathematical Physics, Rutgers University, Piscataway, New Jersey 08854, USA*
[3]*Department of Nuclear Engineering and Radiological Sciences, University of Michigan, Ann Arbor, Michigan 48109, USA*
[4]*Physics and Electronics Directorate, AFOSR, Arlington, Virginia 22203, USA*

Space charge effects reduce electron emission by altering the surface barrier via two effects: increasing the barrier height (Schottky factor) and width to electron emission by lowering the surface field and changing the magnitude of the dipole associated with electron density variation. A one-dimensional emission model using a transit time argument to account for charge in the anode-cathode (AK) gap and an analytical model of the dipole is used to approximate the effects of each factor on the current density. The transit time model is compared to the experimental data of Longo [J. Appl. Phys. **94**, 6966 (2003)] for thermal emission. Changes in the dipole contribution are primarily associated with tunneling and therefore field emission. The transit time plus dipole modification is compared to the experimental data of Barbour *et al.* [Phys. Rev. **92**, 45 (1953)] for field emission. The model's application to thermal-field, and photoemission in general is discussed, with the former corresponding to continuous current limit and the latter to a pulsed current limit of the model. © *2012 American Institute of Physics*. [http://dx.doi.org/10.1063/1.3692577]

I. INTRODUCTION

Space charge limited flow when the dimensions of the anode-cathode (AK) gap are of nanoscale dimensions is of intrinsic theoretical interest given its dependence on electrodynamic, quantum, and even relativistic effects.[1] It is increasingly important in vacuum nanoelectronics devices where quantum mechanical tunneling becomes linked to space charge forces by the latter's effect on the tunneling barrier: in the quantum limit, the relationship between the voltage across a gap and the maximum charge that can be sustained across it departs from the classical Child-Langmuir (CL) relation between anode potential, anode-cathode (AK) gap distance, and the current density. Space charge is commonly understood to reduce emission by reducing the extraction field at the surface of the cathode, eliminating it altogether or even changing its sign so that a potential energy maximum (or, alternately, a potential minimum) appears outside the surface of the cathode: The development of the CL relation assumes that enough charge has been emitted so that the field at the surface vanishes ($V(0)$ and $\partial_x V(0)$ vanish), so that additional charge creates a barrier.

There is another mechanism related to electron penetration into the tunneling barrier and its creation of a dipole contribution to barrier height that also affects current density and is also field dependent. It is the aim of this study to provide simple models that can account for these effects and assess their relative magnitude.

In a one dimensional (or parallel plate) model, when the charge in the gap is sufficient to suppress the field at the cathode surface, when the electron is emitted from the surface with a vanishing velocity, and when the electron behavior is classical, the limiting current is[2,3]

$$J_{CL}(\varphi_a, D) = \frac{4\varepsilon_o}{9}\sqrt{\frac{2q}{m}}\frac{\varphi_a^{3/2}}{D^2}, \qquad (1)$$

where φ_a is the anode potential (so that $q\varphi_a \equiv V_a$ is a potential energy), D is the AK separation, and other factors are as defined in Table I. Extensions to account for non-zero initial electron velocities, finite cathode size, and other physical effects are involved but available.[4] When the barrier to emission is such that a tunneling current contribution is possible, a quantum mechanical treatment[1,5] demonstrates that the CL relation must be modified (when the anode-cathode gap is nanoscale, Lau, *et al.* found that CL limit can be exceeded), and experimental evidence suggests that the CL relation in fact undergoes modification for "nanogaps".[6] More recently, the 1D CL relation has been extended to treat Coulomb-blockade, which occurs for nanoscale dimensions in the few electron regime.[7] Theoretically, when tunneling is important (*e.g.*, field emission) the current is very dependent on the surface field with consequences for the maximum field emission current that can be drawn, as shown by exact treatments for field emission in one dimension.[8,9] Time-dependent phenomena induced by structure on the beam for which space charge is a contributor or a cause is revealed in numerical simulations and experiments for beam parameters characteristic of accelerators and high frequency microstructures.[10–15]

Field emission entails additional complications because fields on the order of GV/m are required. Emission is from two dimensional ("knife-edge") and three dimensional ("conical") structures so as to exploit geometrical field enhancement effects for their attainment. Understanding space charge effects in such circumstances has a long history[16,17]

a)Electronic mail: kevin.jensen@nrl.navy.mil.

TABLE I. Fundamental and other constants expressed in units of [q, nm, fs, eV]. The current density terms use Amp = 6241.5 q/fs.

Symbol	Definition	Value	Unit
q	Unit (electron) charge	1	q
c	Speed of light	299.792	nm/fs
m	Mass of electron	0.056 856 3	eV/c^2
k_B	Boltzmann's constant	1/11 604.5	K/eV
$\hbar$	Planck's constant	0.658 212	eV/fs
α	Fine structure const.	1/137.036	–
ϵ_0	$q^2/4\pi\alpha\hbar c$	0.055 263	q^2/eV nm
Q	$\alpha\hbar c/4$	0.359 99	eV nm
a_o	$\hbar/\alpha mc$	0.052 918	nm
A	$q/16\pi^2\hbar$	1.5414×10^{-6}	Amp/eV
B	$4\sqrt{2m}/3\hbar$	6.8309	1/nm-eV$^{1/2}$
A_{RLD}	$2qm\,(k_B/2\pi\hbar)^2$	120.17	Amp/K^2 cm^2

particularly as such phenomena are thought to relate to breakdown in vacuum nanoelectronic field emitter arrays[18,19] and because such factors impact the behavior of high brightness beams for particle accelerators and vacuum electronic devices.[20–22] Although stylized geometries allow for elegant analytical solutions to determine "beta factors" (how much greater the surface field is than the background field) the incorporation of space charge modifications has remained challenging[4,23] particularly because tractable geometries that can be treated are idealized compared to physical emitters that exhibit nanoscale protrusions, surface contamination, crystal face variation, and asymmetry.

It would be premature to conclude, however, that little of interest remains in the one dimensional model, particularly for small AK gaps and high currents.[6,24–27] In almost all the studies, however, the height of the emission barrier (the work function if measured from the Fermi level, or the electron affinity if measured from the conduction band minimum) is treated as a theoretical input parameter, allowing the space charge fields to modify it only by changing the effective field at the surface (thinning the barrier) or via the Schottky factor (lowering the barrier) for the image charge potential used to model metals[28,29] (Eq. (22) below; Q is modified by a dielectric constant for semiconductors[30]). Specifically, an effect of purely quantum mechanical origin further affects the emission barrier and is caused by variations in electron density near the surface:[31,32] It will be described in greater detail separately[33] but the findings shall be used here. The effects on current density will be of importance when barriers are low (low work function or electron affinity), the AK distance is small, the Fermi level small, or combinations thereof. If analytical or semi-analytical models are desirable, and they are for developing emission models for beam simulation codes, then there is a need for quantitative models of a simplicity that enables the effects to be jointly considered. Below, a transit time model of space charge dominated current is presented and validated, upon which a dipole modification is considered. The most common electron emission mechanisms of field, thermal, and photoemission are contrasted in the framework of the model.

The organization is as follows. First, a model of the 1D space charge problem that allows for an approximate realization of the CL limit is developed but which provides the basis for the emission analysis, and thermal, field, and photoemission processes are considered in light of it. Second, variations in the electron density that give rise to modifications in the emission barrier are summarized. Third, a self-consistent current density/surface field relationship is determined. Lastly, the model is compared and contrasted with experimental data for thermal and field emission: in the former, the model is shown to match a phenomenological account of the transition from space charge dominated to space charge limited flow for dispenser cathodes,[34] and in the later, the 1D approach is contrasted to a discrete charge 3D model to compare to experimental data from a tungsten wire tip with a low work function coating.[17] A discussion of the utility of the model is given (see Table II).

II. SPACE CHARGE, FIELD, AND TRANSIT TIME

A. Distribution function

Under equilibrium conditions, the quantum mechanical current density J past a barrier is constant, and the equations describing thermal, field, and photoemission are obtained from a quantum mechanical treatment of transmission over and through the surface barrier. The paradigmatic triangular barrier potential profile considered by Fowler and Nordheim[35] to characterize field emission provides an exact method to treat field (below barrier) and thermal (above barrier) emission using Airy function solutions to Schrödinger's equation,[32,36,37] a manner of speaking that shall be retained here even though, as argued by Forbes and Deane, "tunneling" and "fly-over" are far more accurate and likely preferable descriptors. Schottky barrier lowering, which rounds the triangular potential, was treated by Murphy and Good[28] in a formulation of field and thermal emission that remains widely used and useful, upon which modifications can be appended.[38]

TABLE II. Emission barrier parameters typical of field emission (material parameters are for copper).

Symbol	Definition	Value	Unit
Φ	Work function	4.5	eV
ϕ	Schottky lowered Φ	$\Phi-\sqrt{4QF}$	eV
μ	Chemical potential	7	eV
x_o	Location of $V(x)$ maximum	$\sqrt{Q/F}$	eV
y	Elliptical argument	$\sqrt{4QF}/\Phi$	–
β	Inverse temperature	$1/k_BT$	eV
V_a	$q \times$ Anode potential	F_oD	eV
F	$q \times$ surface electric field	–	eV/nm
F_o	$q \times$ gap electric field	V_a/D	eV/nm
ρ	Volume number density	–	#/cm^3
σ_o	Sheet number density	–	#/cm^2
τ_o	Space charge free transit time	$\sqrt{2mD/F_o}$	fs
τ	Transit time	Eq. (6)	fs
β_o	Field enhancement factor	$\approx 10^2 - 10^3$	–
D	Anode-cathode separation	–	μm

For all that, an understanding of the transit time model is nevertheless more natural when introduced by a distribution function approach (which is equivalent to approaches to J based on Schrödinger's equation.[39–41]) In one dimension, the Wigner distribution $f(x, k; t)$ satisfies

$$\partial_t f = -\frac{\hbar k}{m}\partial_x f + \int_{-\infty}^{\infty} V(x, k - k')f(x, k'; t)dk', \quad (2)$$

where the function $V(x, k - k')$ accounts for non-local (and in particular, tunneling) behavior. The zeroth, or k^0 moment, of the distribution function is identified with number density ρ, whereas the first, or k^1 moment, is related to the (charge) current density J, apart from a coefficient of $(q\hbar/m)$. An integration over k of Eq. (2) and the antisymmetry in k of $V(x, k)$ results in the continuity equation $q\partial_t\rho = -\partial_x J$. The average velocity is (compare Eq. (4) below)

$$\langle v \rangle \equiv \frac{\int_{-\infty}^{\infty}\frac{\hbar k}{m}f(x,k)dk}{\int_{-\infty}^{\infty}f(x,k)dk} = \frac{J}{q\rho}. \quad (3)$$

Although the Wigner function is good for the evaluation of $\langle v \rangle$ and ρ, the reliance on numerical methods to do so undercuts its ability to model J, as current density is related to the asymmetry of a mostly symmetric distribution function (for metals), and therefore the numerical error associated with finite difference methods overwhelms the exponentially small value of J. For current density, then, $f(x, k)$ is more profitably related to the product of the transmission probability $D(k)$ and the supply function $f_o(k)$ using the more standard Schrödinger-based methods. Nevertheless, Eq. (3) is useful in understanding transit time.

Transit time refers to the passage of electrons from cathode to anode. As far as time scales are concerned, the emission time associated with tunneling is rapid[27] compared to typical AK transit times. Two limits are relevant. The first is characterized by emission current that is constant over time, and the second by emission current that is pulsed (even though each pulse is long in comparison to the tunneling time, although short compared to the transit time across the AK gap).

B. Constant current transit time

When the distribution of charge, or number density, is constant in time, then by the continuity equation, the current density is spatially constant, or $J(x, t) = J_o$. The term $\langle v \rangle$ is the mean velocity of the emitted electrons from Eq. (3): it is, for example, estimated for thermal emission at $x = 0$ by

$$\langle v(0) \rangle \approx \frac{\int_0^{\infty}(\hbar k/m)e^{-\beta E}dk}{\int_0^{\infty}e^{-\beta E}dk} = \sqrt{\frac{2k_B T}{\pi m}}, \quad (4)$$

where $E = (\hbar k)^2/2m$. Because tunneling is involved, an equivalent for field emission is more nuanced: as the electron

emerges from the tunneling barrier, its kinetic energy is of the size of the Fermi energy μ. Compare this initial velocity to the velocity even a short distance away from the cathode surface: the electron acquires an energy comparable to the potential drop near the extraction grid (thermal emission) or gate (field emission) and is therefore larger than several hundred eV. Conditions for photoemission are comparable. It is therefore convenient to neglect the initial velocity in what follows.

Generally, the definition of "transit time" is not unique, but one of two is used here. The ballistic or space-charge-free transit time τ_o is given by the simple relation

$$\tau_o = \sqrt{\frac{2mD}{F_o}} \quad (5)$$

characteristic of motion in a constant field $F_o = V_a/D$. When space charge is present, τ shall be defined by

$$\tau \equiv \int_{x_+}^{D}\frac{dx}{\langle v \rangle} = \frac{q\sigma(D)}{J}, \quad (6)$$

where $x_+(E)$ is the location where the electron of energy E emerges through or over the potential, but which is small compared to D and therefore which shall be treated as negligible. The factor $\sigma(x)$ is defined by

$$\sigma(x) = \int_0^{x}\rho(x')dx'. \quad (7)$$

From Poisson's equation, the potential energy $V(x)$ in the gap region subject to the conditions $V(0) = 0$, $V(D) = V_a$, and $\partial_x V(0) = F$ is

$$V_a = FD + \frac{q^2}{\varepsilon_0}\int_0^{D}\sigma(x)dx \quad (8)$$

$$\equiv FD + \frac{q^2 D}{\varepsilon_0}N_\tau\sigma(D), \quad (9)$$

where N_τ is of order unity and is defined by $N_\tau \equiv \int_0^{D}\sigma(x)dx/(D\sigma(D))$.

The calculation of N_τ is made by rewriting Poisson's Equation as $d[F(x)^2] = (2qJ/\varepsilon_0 v(x))\ dV(x)$. The velocity v is given by $v(x) = [2(V(x) + E_o)/m]^{1/2}$ where $mv_o^2/2 = E_o$ is the initial kinetic energy (KE). A simple integration gives

$$F(x) = \left\{\frac{2q\sqrt{2m}}{\varepsilon_0}J\left[\sqrt{V(x) + E_o} - \sqrt{E_o}\right] + F^2\right\}^{1/2}, \quad (10)$$

where F without an argument is the field at the surface, or $F \equiv F(0)$. A second integration can be performed to obtain a self-consistent relation, as done in Refs. 8 and 9, but here, the intention is to identify the transit time. If the initial kinetic energy $E_o = 0$, then

$$F(x) = \left(F^2 + \frac{2q}{\varepsilon_0}J\sqrt{2mV(x)}\right)^{1/2} \quad (11)$$

and is identical to Eq. (6) of Ref. 9. From $\sigma(D) = (\varepsilon_o/q^2)$ $((V_a/D) - F)$ (see also Eq. (15) below) it follows

$$\tau = \frac{\sqrt{8mV_a}}{F}\left[1 + \left(1 + \frac{qJ}{\varepsilon_o F}\sqrt{8mV_a}\right)^{1/2}\right]^{-1}. \quad (12)$$

Observe that, as expected, the transit time decreases as the field at the surface F increases. From Eqs. (6)–(8),

$$\frac{V_a}{D} \equiv F_o = F + \frac{q}{\varepsilon_o}N_\tau J\tau. \quad (13)$$

As $N_\tau J\tau$ is the average charge per unit area within the gap, the form of Eq. (13) is as expected, and it will serve as the defining equation relating transit time to current density. It is dependent on the force exerted by a charged sheet being independent of distance to the charged sheet. In contrast, for 2D and 3D charge distributions, the field varies as the inverse distance to a power and therefore the calculation of a characteristic time τ would be more difficult: the transit time introduced by Eq. (13) is applicable only in a planar 1D geometry.[42]

Because an exact analytic solution relating $J(F)$ to F exists,[8,9] N_τ may be computed, but the present aim is to consider the adequacy of the transit time approximation and how it fares. Therefore, consider a less exact but more intuitive approach. Space charge limited current arises when F in Eq. (13) vanishes, for which $J \rightarrow J_{CL}$. Consequently, N_τ may be estimated given the transit time approximation used. For $\tau \rightarrow \tau_o$ as in Eq. (5), it follows $N_\tau = 9/8$, as first found in Ref. 3. In contrast, if Eq. (12) is used for τ, then $N_\tau = 3/4$ when $F \rightarrow 0$. Certainly, the usage of τ_o underestimates the influence of space charge, but the $F = 0$ limit of Eq. (12) overestimates it. Therefore, the usage of both in Eq. (13) serves to easily identify when space charge effects become significant. This shall be more apparent when field emission data is considered below (the thermal emission data is at constant anode potential, and therefore, such considerations are subsumed).

C. Pulsed current transit time

When a large amount of charge is instantaneously injected into the AK gap then the density can be modeled as a delta function, or $\rho(x) = (\sigma/D)\delta(x - \bar{x}(t))$, where $x(t)$ is the location of the charged sheet and σ is the charge per unit area of the sheet. Space charge limited flow for such conditions takes on a time-averaged character and simulation is necessary[43] but some assessment can be made of behavior. When charge in the thin sheet is enough to eliminate the field on the cathode, then $\sigma \rightarrow \sigma_o$ and $q^2\sigma_o = J\delta t = \varepsilon_o F_o$, where $\delta t \ll \tau$ is the very short duration of the laser pulse injecting the charge. Emitted charge density in excess of $J\delta t$ will be pushed back to the cathode. The location of the charged sheet is determined by (compare Eq. (1) of Griswold *et al.* in Ref. 43)

$$V_a = F_+(D - \bar{x}) + F_-\bar{x}, \quad (14)$$

where F_- is the field between the cathode surface and the sheet, and F_+ between the sheet and anode: the two generally are not equal, but can be related further by applying Gauss's law to the sheet (*aka* Gaussian pillbox argument). For an arbitrary sheet charge density σ we have

$$\frac{q^2}{\varepsilon_0}\sigma = \mathbf{F}_+ \cdot \hat{n}_+ + \mathbf{F}_- \cdot \hat{n}_- = F_+ - F_-, \quad (15)$$

where $\hat{n}$ are normal to the pillbox surface: on the "$-$" side, the force and the normal are antiparallel. Solving Eqs. (14) and (15) simultaneously gives

$$F_+(\bar{x}(t)) = F_o + \frac{q^2\sigma}{\varepsilon_o D}\bar{x}(t) \rightarrow F_o\left(1 + \frac{\bar{x}(t)}{D}\right), \quad (16)$$

$$F_-(\bar{x}(t)) = F_o - \frac{q^2\sigma}{\varepsilon_o}\left(1 - \frac{\bar{x}(t)}{D}\right) \rightarrow F_o\frac{\bar{x}(t)}{D}, \quad (17)$$

where the arrows correspond to $\sigma \rightarrow \sigma_o$.

The force under which $\bar{x}$ evolves is the average of F_+ and F_- (not their sum, as perhaps thought: in the limit of vanishing σ the fields on each side are equal to F and the field on the sheet is likewise F), and so

$$\frac{d^2}{dt^2}\bar{x}(t) = \frac{F_o}{2mD}(D + 2\bar{x}(t)), \quad (18)$$

with a general solution given by

$$\bar{x}(t) = \frac{D}{2}(\cosh(at) - 1) + \frac{v_o}{a}\sinh(at), \quad (19)$$

where $v_o = \sqrt{2E_o/m}$ is the initial velocity, $a \equiv \sqrt{F_o/mD} = \sqrt{2}/\tau_o$ and $\tau_o = \sqrt{2mD/F_o}$ is the space-charge-free transit time. For photoemission from, *e.g.*, metals, the kinetic energy E_o of the emitted electron is approximately the difference between the photon energy and the barrier height, or $E_o = (1/2)mv_o^2 \approx \hbar\omega - \phi$ if the electron is excited from the Fermi level, and therefore E_o is on the order of a few eV, compared to $V_a \sim 10\,\text{keV}$. The transit time is then the $v_o \rightarrow 0$ transit time from which a small correction is subtracted, or $\tau - \delta\tau$. The $v_o = 0$ transit time τ is

$$\tau = \frac{1}{a}\cosh^{-1}(3) = 1.2465\tau_o, \quad (20)$$

while the correction $\delta\tau$ is

$$\delta\tau = \frac{2\sqrt{E_o}}{3\sqrt{E_o} + \sqrt{V_a}}\tau_o \quad (21)$$

or $0.02\tau_o$ if $E_o \approx 10^{-4}V_a$, so that $\tau - \delta\tau$ is some 20% larger than the space charge free transit time. Estimates using τ_o therefore are approximately adequate for pulsed emission conditions as well.

III. ELECTRON EMISSION

A. Thermal, field, and photoemission

The current J has not been specified, but thermal, field, and photoemission are candidates. For an image charge barrier defined by

$$V_{img}(x) = \mu + \Phi - Fx - \frac{Q}{x}, \qquad (22)$$

$$= \mu + \phi - Fx\left(1 - \frac{x_o}{x}\right)^2, \qquad (23)$$

where the second line explicitly shows the quadratic nature of the potential near the location of its maximum at x_o and where $\phi(F)$ is the Schottky lowered barrier height. Note that Eq. (22) is for the quantum mechanical evaluation of the transmission probability that is required for the calculation of current density. $V_{img}(x)$ is not directly equivalent to $V(x)$ appearing in Eq. (10) that governs electron dynamics in the AK gap—an example of the difference being that $V_{img}(x)$ is measured with respect to the conduction band minimum of the metal and is applied to within several nanometers of the surface, whereas $V(x)$ is measured with respect to the grounded cathode surface and is applied between cathode and anode.

Electrons can be emitted over the barrier $V_{img}(x)$ by having sufficient thermal energy (Richardson-Laue-Dushman[44]); through $V_{img}(x)$ by quantum mechanical tunneling if the barrier is sufficiently thin to a Fermi level electron (Fowler Nordheim[35]); or by being photoexcited (Fowler-Dubridge[45]). For the evaluation of current density herein, the General Thermal-Field-Photoemission equation[46,47] is used (but see Ref. 33 for how it is presently treated). In the appropriate limits it reproduces the more conventional equations, *e.g.,* for thermal emission,

$$\lim_{n\to 0} J_{GTF} = J_{RLD} = A_{RLD}T^2\exp(-\phi/k_BT), \qquad (24)$$

whereas for field emission (after Murphy and Good[28]),

$$\lim_{n\to\infty} J_{GTF} = J_{FN} = A\frac{F^2}{\Phi t(y)^2}\exp\left(-B\frac{\Phi^{3/2}}{F}v(y)\right), \qquad (25)$$

where $n = \beta_F/\beta_T$ is a ratio of energy slope factors found in the transmission probability and supply function, respectively, and $v(y)$ and $t(y)$ are elliptical integral functions for which approximations by Deane and Forbes[48] are convenient. For photoemission,

$$J_{FD} = \frac{q}{\hbar\omega}(1 - R(\omega))F_\lambda P(\hbar\omega)I_\lambda, \qquad (26)$$

where I_λ is the laser intensity (in units of W/cm^2), $R(\omega)$ is the reflectivity, and F_λ is a factor accounting for losses due to scattering. The factor $P(\hbar\omega)$ is the probability of emission which is relatable to the functions defining J_{GTF} but which can be reasonably approximated as $U[\beta(\hbar\omega - \phi)]/U(\beta\mu)$ where $U(x) \approx x^2/2 + (\pi^2/6)$ is the Fowler-Dubridge function.[45] Although all three are derived from or related to J_{GTF}, each cathode technology entails additional considerations (*e.g.,* crystal face, field enhancement, laser intensity, etc.) in order to compare theory to experiment.

B. Continuous and pulsed classification

Thermal emission is the quintessential example of "constant current emission": electrons are boiled off the

surface of the metal, and in the comparatively weak (of order 1 MV/m) fields, F under conditions of "space charge limited current," is either zero or such that a potential hump appears just outside the surface that electrons must surmount to begin their flight to the anode.[2]

At the opposite end, photoemission is governed by the profile of the drive laser pulse, which can be high intensity, flattop, exceptionally short (*e.g.,* intensities of GW/cm^2 over durations of < 500 fs,[49] and with high repetition. Some free electron lasers require current densities in excess of kA/cm^2 so that charges from 0.1 to more than 10 nC can be extracted in 100's of fs to 10's of ps.[50–52] Electrons liberated by photoemission will return to the photocathode if the extraction field is eliminated by space charge: fields associated with a disk containing a nC of charge distributed over mm^2 areas are of the size 113 MV/m, or comparable to the fields supported within an rf photoinjector. Even if emission is not completely suppressed *per se*, structure will be put on the beam that persists[53,54] or affects the bunch.[14] Therefore, short duration, high intensity, rapid photoemission bunches are closer to the pulsed emission classification.

Field emission occurs under the highest fields on the order of 4–10 GV/m, with current densities in excess of 10^8 A/cm^2 at the emission site, and so because J_{FN} can be orders of magnitude in excess of J_{CL}, it may be thought that sufficient charge can be injected into the AK gap to suppress the surface field in a fraction of the transit time τ. For example, if it is naively assumed that for a small time increment δt over which the emission current J is approximately linear in F, then F is reduced by an amount

$$\delta F = \frac{q}{2\varepsilon_0}[J(F) + J(F - \delta F)]\delta t. \qquad (27)$$

That this is misguided is seen as follows. Solving for δt for a fixed δF and adding the increments gives an approximation for $F(t)$, which can be used to examine the behavior of $J(t)/J(0)$. Doing so for copper-like parameters using Eq. (25) for even a small (10 μm) AK gap shows that most of the current would appear to be emitted early after the anode is instantaneously turned on, as in Fig. 1. However, an instant turn-on of the anode is unphysical: unlike photoemission, the current density is dictated wholly by the extraction field, and rise/fall times of the fields are therefore limited by the manner in which the field is created (*e.g.,* for arrays, charging and discharging the gate is limited by capacitive effects[55–57] so that modulation frequencies are limited to be between 10 and 100 GHz frequencies, and rise/fall times are picoseconds in duration).

As field-emitted electrons can span AK gaps of 10's of μm's in under a picosecond, the field at the surface will be reduced by charge distributed throughout the AK gap before the anode potential can be brought to its intended magnitude. Therefore, field emission is well-described by steady state solutions of the 1D field emission problem.[8,9] The interest in field emission is, first, in its strong dependence on the surface field, well in excess of thermal or photoemission (in other words, field emitter arrays, or FEA's, have a very large transconductance by comparison to thermionic cathodes,[55] and
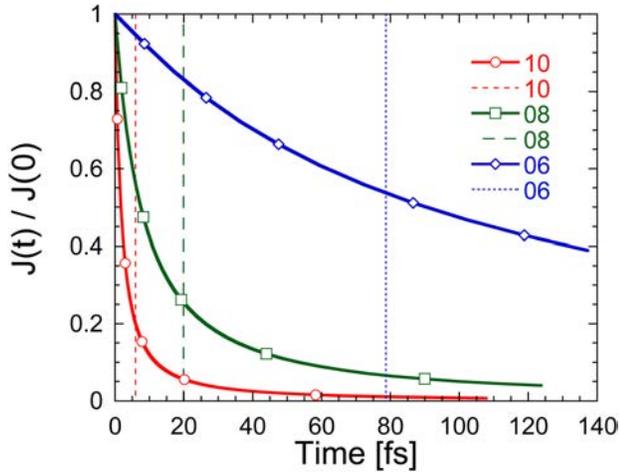
FIG. 1. (Color online) Approximate decline in the field emission current density as a fraction of its initial value as a function of time for copper-like parameters. The solid lines terminate at the approximate transit time for each field (given by the number labeling each line in [eV/nm]). The dashed line corresponds to the emission time if the current were constant and equal to its initial value. Copper-like material parameters, the general thermal-field emission equation J_{GTF}, and an AK separation of $10\mu m$ are used.

the dependence of $P(\hbar\omega) \propto (\hbar\omega - \Phi + \sqrt{4QF})^2$ on F for photoemission is comparatively weak), and second, the dipole modification to Φ is most apparent at high fields where field emission dominates. As a result, space charge effects in field emission requires additional considerations.

IV. THERMAL EMISSION ANALYSIS

A. The Longo equation

A well known empirical relation due to Longo[34] used in life-test models of barium dispenser cathodes anticipates the change in behavior that occurs when $F \to 0$ in the case of thermal emission, and serves to qualify Eq. (13) in the thermal limit. Generalizing from Eqs. (1) and (7) of Ref. 34, the current density J from dispenser cathodes follows the form

$$\frac{1}{J^\alpha} = \frac{1}{(J_{RLD})^\alpha} + \frac{1}{(J_{CL})^\alpha}, \qquad (28)$$

where α was designated by Longo as a "shape factor" (Eq. (1) of Longo corresponds to $\alpha = 1$) said to govern how quickly J transitioned from J_{RLD} to J_{CL} and was argued to be based on work function evolution due to coverage. Vaughan[58] was less sanguine about interpretation, asserting, first, that α (his n) had no theoretical justification but was merely a fitting parameter, and second, that "good" cathodes are characterized by $6 \leq \alpha \leq 10$. Because J_{RLD} is an exponentially increasing function of temperature, an addition of inverses behavior allows the smallest current to dominate: For low temperatures, it will be the RLD current (source limited), whereas at high temperatures, it will be the CL current (space charge limited). For increasing α, the transition is increasingly sharpened: Therefore, Vaughan argued, its value functions as a fitting factor governing the smoothness of the "knee" of the transition.

Explanations of the "knee" behavior typically include (but are not limited to) variations of three factors: (*i*) As

Longo argued, evolution of the cathode changed the degree of coverage and therefore the work function (as per Gyftopoulos-Levine theory[32,59]); (*ii*) emitted electrons have a thermal spread in launch velocity, whereas initial velocities are neglected in Eq. (12); (*iii*) sintered dispenser cathodes exhibit a multitude of crystal faces, each of which has a characteristic barium lowered work function and that therefore causes non-uniform current density near the surface of the cathode. Such factors introduce velocity spread into the beam that in turn cause a spread in transit times, by creating changes in the accelerating field near the surface of the cathode.

Two additional observations affect such explanations. First, the length scale of variations in Φ limits the length scale over which changes in the field near where the cathode occur and therefore are comparable to pore-to-pore separation and crystal grain size (on the order of $10\,\mu m$ for standard dispenser cathodes for those pores furthest apart, and $6\,\mu m$ for the average grain size[60]). Consequently, the length scales over which different surface fields operate below the space charge limit is then of a similar size:[9] compare to the usual AK gap length that is more than $100\times$ larger. Therefore, spreads in transit time introduced by velocity differences related to non-uniformity do contribute, but because the bulk of the transit trajectory is in regions beyond the influence of non-uniformity, such explanations must likely be augmented to explain the full behavior of the knee region between the thermal and space charge current densities observed in Fig. 2.

Second, the finite size of the cathode emission area in comparison to the AK gap will matter: the beam cross section will expand and thereby soften the 1D space charge limit dependent on how large the beam diameter is compared to the AK gap (the infinite B-field approximation is used to restrict this effect[61]). Represent the emission region of the cathode as a disk of radius R at a distance D away. Using the method of images, the equipotential surfaces are represented by the cathode disk plus its image reflected through the anode plane at a distance $2D$ away. The potential energy on
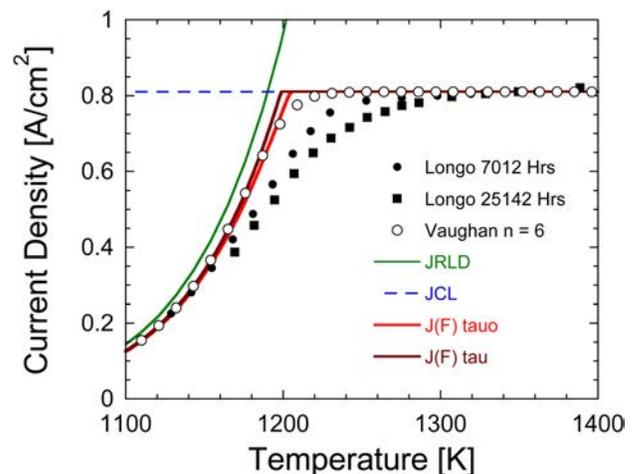

FIG. 2. (Color online) Current density from a Ba dispenser cathode (Fig. 4 of Longo[34] for two different ages of the cathode (black dot and square), and an $\alpha = 6$ curve for Vaughan's "good cathode" (black open dot) compared to $J = J_{RLD}$ (green left-most line) and J_{CL} (dashed blue line). The adjacent theory lines $J(F)$ use τ_o and τ (right and left overlapping lines, respectively) in solving Eq. (13).

axis $q\varphi(z)$ is approximately a sum of ring charges representing the cathode and its image. Introduce the dimensionless terms $r = R/D$ and (to reflect the symmetry about the anode) $z(u) = D(1 + u)$ to find

$$\frac{q\varphi(z(u))}{V_a} = 1 + \frac{g_r(u)}{\sqrt{r^2 + 4} - r - 2}, \tag{29}$$

where

$$g_r(u) = 2u + \sqrt{r^2 + (1 - u)^2} - \sqrt{r^2 + (1 + u)^2}. \tag{30}$$

For large r, $\phi(z)$ is approximately linear in u (and therefore z) but when the radius of the cathode approaches the AK separation ($r \approx 1$) non-linear behavior in u is apparent. Thus, acceleration near the anode is smaller than near the cathode, and so the transit time increases compared to the $r \to \infty$ (*i.e.*, 1D) limit. In addition, for electrons emitted off-axis, the path lengths are longer (a portion of the kinetic energy from the potential change is in the transverse components and so the paths acquire an arc-like appearance), indicating that the current density of the beam decreases as the beam expands, an effect which becomes progressively larger as the edge of the cathode is approached. Axial forces associated with space charge will contribute further to the arcing of the trajectories. Consequently, a range of transit times invariably occurs when $r \lesssim 1$. Near the space charge limit, electrons are pushed away from the axis of symmetry, the path lengths increase, and the transit times grow. A correlated effect is the introduction of oscillations within the finite-sized emission pulse that have been revealed in Particle-in-Cell, or PIC, simulations explicitly.[13] These effects depend on how close to the cathode edge the launch site of the electron is. In aggregate, a range of transit times will likely contribute to the softening of the sharp transition implied by Eqs. (13).

B. Comparison to experiment

The consequences of Eq. (13) are now compared to the Longo empirical model. When $F > 0$ then $J = J_{GTF}(T, F_o) \approx J_{RLD}(T)$ but when F vanishes, $J = J_{CL}$. The effect of the extraction field is felt in the changes wrought by the Schottky factor $\sqrt{4QF}$ on Φ. Using J_{GTF} with barium on tungsten material parameters ascertained from the low-T behavior ($\mu = 11$ eV, $\Phi = 1.98$ eV, $V_a/q = 36.125$ Vs, and $D = 250 \,\mu$m, where the last two parameters are typical of dispenser cathodes but not necessarily identical to the (unreported) values of the experiment) under the assumption that 88% of the surface is actively emitting specifies the theoretical model (the factor N_τ is subsumed in the "active area" approximation).

Predictions of the theoretical model for both transit times are shown alongside Longo's data (closed circles and squares) in Fig. 2 (τ_o corresponding to red (to the right) and τ to brown (to the left), solid lines). Vaughan's "good cathode" value of $\alpha = 6$ is also shown (open circles)—parenthetically, values of $\alpha = 1.8$ and 2.5 characterize the 7012 Hrs and 25 142 Hrs lines, respectively. Observe that the $J_{GTF} \approx J_{RLD}$ line (green solid left-most line) is without the 88% active area factor for comparison. It is clear that a space charge

reduction of the field at the surface in the transit time model anticipates the shape of the data: while theory will not explain the behavior in the knee region for $\alpha = 1$ (as per Longo), it does anticipate the trend nicely for $\alpha \approx 6$ (as per Vaughan).

V. FIELD EMISSION ANALYSIS

A. Transit time for field emission

For field emission, charge will always be present in the gap and so the initial field must always be less than F_o, making the evaluation of the surface F and therefore τ complex. The dependence of the barrier height $\mu + \phi(F)$ on F necessitates an iterative approach (in the present case, a bisection search algorithm is used), complicated further by the fact that Φ is itself is dependent on the distribution of charge at the surface that induces a dipole contribution that must be evaluated from solutions to Schrödinger's equation.[33] Introducing the displacement factor

$$\Delta(F) = \frac{1.4569 \eta(F)}{k_F(1 + \sqrt{1 - \eta(F)})}, \tag{31}$$

where $\eta(F) = 1.1373\pi F a_0/\mu$, then the leading order contribution from the dipole in $\Phi \to \Phi + \delta\varphi$ is

$$\delta\varphi = \frac{8}{9\pi} Q k_F (k_F \Delta)^2 (1.3580 - 0.31072 k_F \Delta). \tag{32}$$

When Φ appears in any of the emission equations, therefore, Eq. (32) is required to augment its value to account for the variation of the dipole induced by a shifting electron density at the surface in response to the changing field F.

B. Comparison to experiment

In a previous study[62], the effect of emitted charge on field emission was analyzed by summing over the contribution of sequentially emitted electrons and that model was compared to the data of Barbour *et al.*[17] for a tungsten needle with a micron-scale radius of curvature on which submonolayer coverings of barium were applied. Although the onset of space charge effects in that model were anticipated, the "turn-over" exhibited by the experimental data was softer than that predicted by the sequentially emitted electron model; additionally, the theoretical model did not contain a dipole modification due to electron density variation. The transit time approach is a conceptually different method of attacking the same problem, but it is hampered by being a 1D model when the data is from an explicitly 3D structure.

A qualitative comparison remains possible: although the transit time analysis is 1D and needles are not, when emitted charge from a needle moves more than a few tip radii away from the emission site, the $1/r^2$ behavior of Coulomb forces reduces the impact of the space charge fields generated by it, and therefore the fading of the field due to emitted charge crudely mimics an absorbing anode. Consequently, the physical reality of emission from a needle conceptually lies between the sequential emission (3D) model and the transit time (1D) model. To the transit time model's

disadvantage, the AK separation is ambiguous when applied to a needle, and because the emitted current from a conical tip scales with current density at its apex, a quantitative comparison inevitably requires the usage of scale factors to compare theory to experiment. This is in contrast to the sequentially emitted electron + Point Charge Model (PCM) representation of the emitter of Ref. 62, from which the field enhancement ("beta" factor β_o) and total current allow for a direct comparison. To the transit time model's advantage, it presumes so-called sheets of charge density that are emitted, which gives an effect hard to account for in a PCM approach by spatially distributing the charge to a sheet and thereby softening the turn over signaling the onset of space charge.

In Fig. 3, theory (Th) relates current density (J) to field (F), whereas experiment (Exp) relates total current (I) to anode potential (V_a). These terms are related by field enhancement factors β_o, emission areas, and the AK separation. The experimental x-axis therefore uses the field $\beta_o V_a$, where the experimental $\beta_o = 4516 q$/cm was determined in Ref. 62: Recall that beta factors relating field to voltage have dimensions of charge over length, whereas beta factors relating apex field to background field are dimensionless. A solid theory line uses Eq. (12), whereas a dashed theory line uses Eq. (5)—the difference between them is more consequential due to the greater impact of field on emission.

It is seen that the theoretical and experimental x-axes differ by a scale factor of < 2, whereas the y-axes differ by a scale factor related to the logarithms of the ratio of the putative emission area ($< 2\pi(364\,\text{nm})^2$) with 1 cm^2 and the fraction of the surface emitting. Nevertheless, once such factors are specified, the good qualitative agreement between the trends in the experimental data and the theoretical predictions, particularly in the transition region and the relative behavior of the different coverage cases, indicate that the space charge forces have a "sheet-like" behavior characteristic of the transit time model and the dipole term increasingly
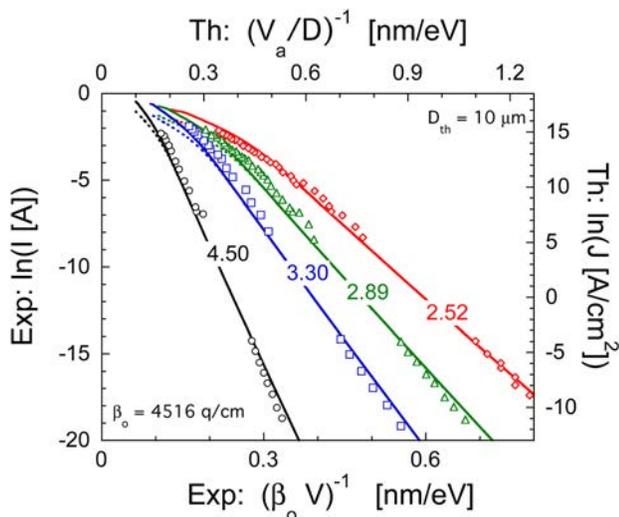

FIG. 3. (Color online) Comparison of the (experimental - symbol) data of Fig. 3 of Ref. 17 to the predictions of the transit time (theoretical - line) model on a Millikan-Lauritsen plot. Numbers after "ln(J)" refer to Φ in eV as calculated using the low anode potential data where field emission does not contribute. The gap in the experimental data reflects the different methods used to collect the data: see Ref. 17.

matters. That the experimental data can be bracketed by different transit time models bodes well for the development of theoretical models that can be utilized by Particle-in-Cell codes[12,63–66] that benefit from a quantitative field emission + space charge model in the treatment of dark current, intrinsic emittance and emission non-uniformity that accompany electron beam formation in particle accelerators and photoinjectors.

VI. CONCLUSION AND DISCUSSION

A one-dimensional analysis of the onset of space charge effects was developed in the context of a transit time model augmented with a dipole due to electron density variation. It was compared to experimental data from two different emission sources, thermionic and field emission. These sources fit into a "continuous emission" model in contrast to photoemission, which is describable by a "pulsed emission" model. The experimental measurements exhibiting the onset of space charge were based on (thermal) barium dispenser cathodes and (field) sharpened tungsten wires increasingly coated with barium. The transit time plus dipole model was shown to capture the relevant physics.

The methodology is not presented as a rigorous or exact treatment of space charge effects—it is not, and analytic treatments or simulations which are already exist. The comparison of the transit time model to available experimental data for conventional thermal emission (dispenser cathode) or field emission (tungsten needle) was to show the model's compatibility with measured data, and therefore validate its usage as a point of departure when conditions are more challenging, as anticipated for photoemission, where time-dependent oscillations within bunches of emitted charge have appeared in simulation.

In particular, the transit time methodology is expeditious to quantify space charge effects when the emission probability is altered, or when the anode-cathode separation is (or may be approximated as) small, or when the supply of electrons contains a significant thermal component (as occurs when temperatures are high or the electron density in bulk is small by comparison to metals, *e.g.,* semiconductors), with or without band bending. In these cases, an accurate treatment of the transmission probability or resolution of the emission process over the relevant time scales in PIC is computationally prohibitive even as it is recognized that fast fluctuations in the emission current may exist and be unavoidable at high current densities. Such issues are already recognized as a source of difficulty in the proper implementation of the emission equations, particularly those for field emission[12,21] and photoemission.[13]

It is argued that the transit time model will be of greater consequence for theoretical photoemission models in development, as photocathode surfaces are flat but have small barriers associated with high quantum efficiency semiconductors (*e.g.*, GaAs, CsK$_2$Sb, and CsTe) for which band bending and dipole modifications similar to Eq. (32) affect emission. Such photocathodes operate under fields intermediate between those characteristic of thermal and field emission considered herein, and the smallness of the barrier implies that the dipole

term will matter to a greater extent. Regarding time dependence, the shape of the pulse is controlled by the laser profile rather than the emission process, and the transport of electrons to the surface contain both fast and long time scales correlated to whether scattering complicates the emission process.[67] Other thermal and field effects may be treated as perturbations to the zero temperature or simple triangular barrier limit. Therefore, photoemission constitutes an extension of the analysis with difficult modifications, making the vetting of the transit time approach with traditional thermal and field emission data a necessary part of its validation. In addition to charge within the AK gap, it has been shown that when barrier penetration is significant, the quantum dipole term contributes non-trivially, an observation of greater consequence for photoemission from semiconductors.

ACKNOWLEDGMENTS

[1] L. K. Ang, W. S. Koh, Y. Y. Lau, and T. J. T. Kwan, Phys. Plasmas **13**, 056701 (2006).
[2] C. K. Birdsall and W. B. Bridges, *Electron Dynamics of Diode Regions* (Academic, New York, 1966), pp. xv, 270 p.
[3] R. J. Umstattd, C. G. Carr, C. L. Frenzen, J. W. Luginsland, and Y. Y. Lau, Am. J. Phys. **73**, 160 (2005).
[4] J. W. Luginsland, Y. Y. Lau, R. J. Umstattd, and J. J. Watrous, Phys. Plasmas **9**, 2371 (2002).
[5] Y. Y. Lau, D. Chernin, D. G. Colombant, and P. T. Ho, Phys. Rev. Lett. **66**, 1446 (1991).
[6] S. Bhattacharjee, A. Vartak, and V. Mukherjee, Appl. Phys. Lett. **92**, 191503 (2008).
[7] Y. B. Zhu and L. K. Ang, Appl. Phys. Lett. **98**, 051502 (2011).
[8] R. Forbes, J. Appl. Phys. **104**, 084303 (2008).
[9] A. Rokhlenko, K. L. Jensen, and J. L. Lebowitz, J. Appl. Phys. **107**, 014904 (2010).
[10] R. Hartman, W. Mackie, and P. Davis, J. Vac. Sci. Technol. B **14**, 1952 (1996).
[11] I. Haber, F. Bieniosek, B. Celata, A. Friedman, D. Grote, E. Henestroza, J. Vay, S. Bernal, R. Kishek, P. O'Shea, M. Reiser, and W. Herrmannsfeldt, Laser Part. Beams **20**, 431 (2002).
[12] Y. Feng and J. Verboncoeur, Phys. Plasmas **13**, 073105 (2006).
[13] J. Petillo, D. Panagos, S. Ovtchinnikov, A. Burke, C. Kostas, K. Jensen, B. Levush, B. Held, J. DeFord, and E. Nelson, in 19.2: Modeling Emission Processes in the Finite- Element MICHELLE Gun & Amp; Collector Simulation Code, Proceedings of the 2010 IVEC, Monterey, CA, 2010, pp. 441–442.
[14] K. Tian, R. A. Kishek, I. Haber, M. Reiser, and P. O'Shea, Phys. Rev. ST Accel. Beams **13**, 034201 (2010).
[15] A. Pedersen, A. Manolescu, and A. Valfells, Phys. Rev. Lett. **104**, 175002 (2010).
[16] W. P. Dyke and J. Trolan, Phys. Rev. **89**, 799 (1953).
[17] J. P. Barbour, W. Dolan, J. Trolan, E. Martin, and W. Dyke, Phys. Rev. **92**, 45 (1953).
[18] K. L. Jensen, M. Kodis, R. Murphy, and E. Zaidman, J. Appl. Phys. **82**, 845 (1997).
[19] F. Charbonnier, J. Vac. Sci. Technol. B **16**, 880 (1998).
[20] E. Nelson and J. Petillo, IEEE Trans. Plas. Sci. **32**, 1223 (2004).
[21] Y. Feng and J. Verboncoeur, Phys. Plasmas **12**, 103301 (2005).
[22] H. Kim, Y. Feng, and J. Verboncoeur, J. Comput. Phys. **223**, 629 (2007).
[23] Y. Y. Lau, Phys. Rev. Lett. **87**, 278301 (2001).
[24] L. K. Ang, Y. Y. Lau, and T. J. T. Kwan, IEEE Trans. Plas. Sci. **32**, 410 (2004).
[25] W. Koh and L. K. Ang, Appl. Phys. Lett. **89**, 183107 (2006).
[26] L. K. Ang and P. Zhang, Phys. Rev. Lett. **98**, 164802 (2007).
[27] M. Kleber, Phys. Rep. **236**, 331 (1994).
[28] E. L. Murphy and R. H. Good, Phys. Rev. **102**, 1464 (1956).
[29] S. Christov, Physica Status Solidi **17**, 11 (1966).
[30] R. Stratton, Phys. Rev. **125**, 67 (1962).
[31] K. L. Jensen, J. Appl. Phys. **85**, 2667 (1999).
[32] K. L. Jensen, in *Advances in Imaging and Electron Physics, Volume 149: Electron Emission Physics*, edited by P. Hawkes (Academic Press, San Diego, 2007).
[33] K. L. Jensen, "A quantum dipole modified work function from a simplified electron emission barrier," J. Appl. Phys. **111**, 054916 (2012).
[34] R. Longo, J. Appl. Phys. **94**, 6966 (2003).
[35] R. H. Fowler and L. Nordheim, Proc. Roy. Soc. London Series A **119**, 173 (1928).
[36] A. Rokhlenko, J. Phys. A: Math. Theor. **44**, 055302 (2011).
[37] R. G. Forbes and J. Deane, Proc. Roy. Soc. London Series A, May 18, 2011.
[38] R. Forbes, J. Appl. Phys. **103**, 114911 (2008).
[39] M. Hillery, R. Oconnell, M. Scully, and E. Wigner, Phys. Rep. **106**, 121 (1984).
[40] Y. S. Kim and M. E. Noz, *Phase Space Picture of Quantum Mechanics: Group Theoretical Approach* (World Scientific, Singapore, 1991), pp. xiii, 334 p.
[41] K. L. Jensen and A. Ganguly, J. Appl. Phys. **73**, 4409 (1993).
[42] Y. B. Zhu and L. K. Ang, private communication September 1, 2011; R. G. Carter, private communication September 1, 2011; P. Zhang and Y. Y. Lau, private communication September 1, 2011.
[43] M. E. Griswold, N. J. Fisch, and J. S. Wurtele, Phys. Plasmas **17**, 114503 (2010).
[44] C. Herring and M. Nichols, Rev. Mod. Phys. **21**, 185 (1949).
[45] L. A. Dubridge, Phys. Rev. **43**, 0727 (1933).
[46] K. L. Jensen, J. Appl. Phys. **102**, 024911 (2007).
[47] K. L. Jensen, Y. Y. Lau, D. W. Feldman, and P. G. O'Shea, Phys. Rev. ST Accel. Beams **11**, 081001 (2008).
[48] J. H. B. Deane and R. G. Forbes, J. Phys. A: Math. Theor. **41**, 395301 (2008).
[49] J. Girardeau-Montaut, C. Girardeau-Montaut, S. Moustaizis, and C. Fotakis, Appl. Phys. Lett. **62**, 426 (1993).
[50] D. H. Dowell, S. Joly, A. Loulergue, J. P. De Brion, and G. Haouat, Phys. Plasmas **4**, 3369 (1997).
[51] J. Lewellen, Proc. of SPIE - Int. Soc. Optical Engineering **5534**, 22 (2004).
[52] *Scientific Assessment of High-Power Free-Electron Laser Technology*, edited by N. R. C. of the National Academies (The National Academies Press, Washington, DC, 2009).
[53] J. Harris and P. O'Shea, IEEE Trans. Elect. Dev. **53**, 2824 (2006).
[54] J. R. Harris, J. G. Neumann, K. Tian, and P. G. O'Shea, Phys. Rev. E **76**, 026402 (2007).
[55] J. Calame, H. Gray, and J. Shaw, J. Appl. Phys. **73**, 1485 (1993).
[56] K. L. Jensen, J. Appl. Phys. **83**, 7982 (1998).
[57] K. L. Jensen, P. G. O'Shea, D. W. Feldman, and J. L. Shaw, J. Appl. Phys. **107**, 014903 (2010).
[58] R. Vaughan, IEEE Trans. Elect. Dev. **33**, 1925 (1986).
[59] E. P. Gyftopoulos and J. D. Levine, J. Appl. Phys. **33**, 67 (1962).
[60] N. A. Moody, K. L. Jensen, D. W. Feldman, E. J. Montgomery, and P. G. O'Shea, J. Appl. Phys. **102**, 104901 (2007).
[61] A. Rokhlenko and J. Lebowitz, Phys. Plasmas **11**, 4559 (2004).
[62] K. L. Jensen, J. Appl. Phys. **107**, 014905 (2010).
[63] J. Petillo, E. Nelson, J. Deford, N. Dionne, and B. Levush, IEEE Trans. Elect. Dev. **52**, 742 (2005).
[64] K. L. Jensen, J. J. Petillo, E. J. Montgomery, Z. Pan, D. W. Feldman, P. G. O'Shea, N. A. Moody, M. Cahay, J. E. Yater, and J. L. Shaw, J. Vac. Sci. Technol. B **26**, 831 (2008).
[65] D. Dimitrov, R. Busby, J. Cary, I. Ben-Zvi, T. Rao, J. Smedley, X. Chang, J. Keister, Q. Wu, and E. Muller, J. Appl. Phys. **108**, 073712 (2010).
[66] J. Petillo, D. Panagos, S. Ovtchinnikov, A. Burke, C. Kostas, K. Jensen, B. Levush, B. Held, J. DeFord, and E. Nelson, Proceedings of the 2010 IVEC, Monterey, CA, 2010.
[67] K. Jensen, E. Montgomery, D. Feldman, P. O'Shea, J. Harris, J. Lewellen, and N. Moody, J. Appl. Phys. **110**, 034504 (2011).